Time-domain photoacoustic spectroscopy of solids

A. Mandelis and B. S. H. Royce

Materials Laboratory, Princeton University, Princeton, New Jersey 08540
(Received 13 October 1978; accepted for publication 8 January 1979)

Most conventional photoacoustic spectroscopy of solids has employed a periodically modulated light source. The availability of high-intensity pulsed light sources of short pulse duration makes possible the study of the time response of a photoacoustic system in which the solid is excited by a single optical pulse. A one-dimensional theoretical model is presented in which the time dependence of the photoacoustic response is evaluated for systems of variable optical absorption coefficient and sample thickness. The analysis is restricted to the case for which nonradiative relaxation processes occur instantaneously on the time scale of the measurement. Typical response curves for optically excited systems are presented and interpreted in terms of physical processes occurring in the cell.

PACS numbers: 78.20.Hp

I. INTRODUCTION

The photoacoustic spectroscopy of solid samples is currently being explored in many laboratories as a tool for measuring the optical properties of specimens on which conventional optical absorption measurements are difficult. The technique is capable of providing information about the nonradiative deexcitation processes that occur after a sample has been stimulated by the absorption of a photon. In the "conventional" photoacoustic spectrometer, the sample is excited by a periodically modulated light beam of controlled wavelength and both the amplitude and phase of the photoacoustic signal produced by the periodic heating of the sample are monitored. In principle, this data enables the optical absorption coefficient of the material to be determined and the phase data may be used to provide information about the relaxation times associated with the nonradiative deexcitation paths. This last measurement is, however, complicated by the fact that the phase also contains a component due to the optical absorption depth of the exciting radiation in the specimen under study and the thermal transit time in this solid. Also, for good phase resolution high modulation frequencies should be employed and these reduce the amplitude of the photoacoustic response.

The theoretical models developed to compute the response of a photoacoustic cell under the conditions described above can be divided into two groups based on the complexity of the thermal transport equation used to describe processes occurring in the gas in contact with the solid being studied. Rosencwaig and Gersho[1,2] and Rosencwaig[3,4] have formulated a model in which a simplified form of the trasport equation in the gas was employed. This model ignores the finite transit time of a pressure wave in the cell taking the pressure to be the same at all points in the cell at each instant. Pressure fluctuations in the cell result from the periodic heat transfer between the sample, heated by the modulated radiation source, and a gaseous layer on the order of a thermal diffusion length in thickness that is in contact with it. The thermal expansion of this boundary layer causes it to act as an "acoustic piston" which adiabatically compresses the gas in the rest of the cell and hence generates the PAS signal. Despite the simplification of the gas transport equation the algebraic expressions obtained for the pressure in the cell are still complex. Certain simplified solutions were obtained for limiting cases which provide direct relationships between the magnitude of the PAS signal and the optical absorption coefficient, linear dimensions and thermal properties of the solid together with the modulation frequency of the light and the thermal properties of the gas in the cell. This model has been frequently successfully employed in the interpretation of experimental data.

The second group of theoretical models follows the early work of Parker[5] and their authors employ a more complete form of the gas thermal transport equation which takes into account the finite velocity of sound but still neglects effects due to viscosity. Aamodt *et al.*[6] applied this method to evaluate the dependence of the photoacoustic signal upon the size of the cell. Whereas the Rosencwaig model is unsuitable for cells having dimensions on the order of a thermaldiffusion length in the gas, the more exact treatment of Aamodt *et al.* enables a self-consistent aproach to cells that are shorter than, or longer than, this thermal diffusion length. In the large cell limit the conclusions of this improved model agree with those of the simpler Rosencwaig and Gersho model. Recently this more complete model has been extended by McDonald and Wetsel[7] to include pressure contributions arising from the thermal expansion of the solid and acoustic-wave propagation within the solid. In certain regions of the optical absorption coefficient and the modulation frequency these additional contributions to the PAS signal become significant but in the range of parameters frequently encountered in PAS measurements this model is also in reasonable agreement with the simpler approach of Rosencwaig.

The availability of pulsed laser light sources suggests that an understanding of the time response of a photoacoustic cell to an excitation pulse would be of value. Quantities such as relaxation times associated with nonradiative decay paths would be expected to be measurable as time delays in this approach although once again the interpretation of the data will be complicated by thermal transport effects due to

 0021-8979/79/064330-09$01.10

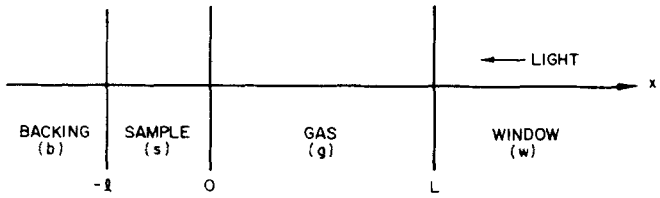

FIG. 1. Schematic Diagram of the one-dimensional cell geometry.

variable optical properties. Surface adsorbates may also be more easily detectable by this method.

Experiments have been reported in the literature in which the time development of a photoacoustic signal following a pulse stimulation was recorded. Callis[8] *et al.* describe the use of a capacitor microphone to detect volume changes resulting from the optical flash excitation of chromatium chromatophores. Callis[9] has also described a piezoelectric calorimeter in which the sample to be investigated is suspended in a transparent solid medium and the pressure pulse generated following optical excitation is detected by a contiguous clamped piezoelectric transducer. Both thermal expansion and acoustic-wave transport contribute to the signal in this case. Farrow *et al.*[10] also report data on the piezoelectric detection of photoacoustic signals generated in a solid deposited on the transducer surface and excited either by a modulated light source or a pulsed argon ion laser. In this case the system is unclamped and the signal should arise from acoustic-wave generation in the solid under study. No intermediate gas pressure transfer medium is involved in these last two cases.

Theoretical exploration of the response of a conventional photoacoustic cell to pulsed excitation has received attention from Aamodt and Murphy.[11] These authors employ the more complete form of the gas thermal transport equation used in their previous study[6] of a cell stimulated by modulated radiation. The response of the photoacoustic system is expressed in terms of its Laplace transform and no examples of analytical inversions are presented. The authors use numerical techniques to evaluate the cell response for the case of a short-duration square temperature pulse and note that this is not the equivalent of the response to a light pulse of corresponding duration because of the different energy distribution in the solid in the two cases and the time dependence of the surface temperature of the solid. Examples are also given where square heating pulses with either a uniform or exponential position dependence in the solid are considered.

This paper presents a treatment of the response of a photoacoustic cell to a pulse of light energy absorbed by a solid sample in the cell. For this case it is the distributed heat input to the solid that is in the form of a Heaviside function rather than the sample temperature. To enable analytical inversions of the Laplace transforms of the pressure in the cell to be made, the simplified form of the gas transport equation is employed. This is equivalent to assuming an infinite velocity of sound but for the cell dimensions considered should give agreement with the more complete model at times on the order or 10^{-5} sec and longer. This is a range of practical interest when a microphone is used as a pressure transducer. The data is discussed in simple physical terms.

II. THEORY

A. Outline of the model

Optical, acoustic, and thermal processes occurring in a photoacoustic cell excited by a light pulse of short duration are treated in a one-dimensional approximation corresponding to the configuration illustrated diagramatically in Fig. 1. A solid of thickness l (cm) having an optical absorption coefficient β (cm^{-1}) is supported on an optically transparent backing. The cell, of length L (cm), contains an optically transparent gas and the light pulse enters the cell through a nonabsorbing window. Both the backing and the window are taken to be thick so that their exterior boundaries are not important. The sample is excited by a light pulse in the form of a Heaviside function of duration τ_p (sec) and an irradiance of I_0(W cm^{-2}). The nonradiative deexcitation processes following light absorption in the solid are taken to be instantaneous. The pressure in the cell (the PAS signal) is assumed to be uniform throughout the cell and to exhibit no delays due to the finite velocity of sound.

Under the conditions outlined above, the thermal diffusion equations for each of the regions of the cell can be written, with only that for the solid containing a distributed heat source for the duration of the pulse. For the solid

$$\frac{\partial^2}{\partial x^2} T_s(x,t) - \frac{1}{\alpha_s}\frac{\partial}{\partial t} T_s(x,t)$$

$$= \frac{-\eta\beta I_0}{K_s}\exp(\beta x), \qquad 0 < t \leqslant \tau_p, \quad -l \leqslant x \leqslant 0,$$

$$= 0, \qquad t > \tau_p, \quad -l \leqslant x \leqslant 0, \tag{1a}$$

where $T_s(x,t)$ is the temperature of the solid, η is the efficiency of the nonradiative processes, K_s is the thermal conductivity, and $\alpha_s = K_s/\rho_s C_s$ is the thermal diffusivity. C_s and ρ_s are the specific heat and density of the solid, respectively.

Three similar equations, but with no source term, hold for the other regions of the cell. These have the form

$$\frac{\partial^2}{\partial x^2} T_i(x,t) - \frac{1}{\alpha_i}\frac{\partial}{\partial t} T_i(x,t) = 0, \qquad \text{for all } t$$

where for

$$x \leqslant -l, \quad i = b \text{ (backing)}, \tag{1b}$$

$$0 \leqslant x \leqslant L, \quad i = g \text{ (gas)}, \tag{1c}$$

$$x \geqslant L, \quad i = w \text{ (window)}. \tag{1d}$$

Since only temperature changes due to the light pulse are of interest, Eqs. (1) are subject to the initial condition: $T_i(x,0) = 0$ and to the condition of temperature and heat flux continuity at the boundaries between the regions for all times.

The time-domain equations (1a)–(1d) are solved in Laplace space s by taking their Laplace transforms. This reduces the partial differential equations in (x,t) to a set of ordinary differential equations in x. The Laplace transforms of Eqs. (1) have the form

$$\frac{d^2}{dx^2}\hat{T}_s(x,s) - \frac{s}{\alpha_s}\hat{T}_s(x,s) = -\left(\frac{\eta\beta I_0}{K_s}\right)\left(\frac{1-\exp(-s\tau_p)}{s}\right)\exp(\beta x), \quad -l \leqslant x \leqslant 0, \tag{2a}$$

and

$$\frac{d^2}{dx^2}\hat{T}_i(x,s) - \frac{s}{\alpha_i}\hat{T}_i(x,s) = 0 \begin{cases} x \leqslant -l, & i = b, \quad (2b) \\ 0 \leqslant x \leqslant L, & i = g, \quad (2c) \\ x \geqslant L, & i = w, \quad (2d) \end{cases}$$

where the $\hat{T}_i(x,s)$ are the Laplace transforms of the temperature distributions in the regions i. Equations (2) are solved subject to the condition that at each boundary

$$\hat{T}_i = \hat{T}_j \tag{3a}$$

and

$$K_i\frac{\partial\hat{T}_i}{\partial x} = K_j\frac{\partial\hat{T}_j}{\partial x} \tag{3b}$$

and yield the following expressions for $\hat{T}_i(x,s)$:

$$\hat{T}_s(x,s) = c_1(s)\exp(-a_s x) + c_2(s)\exp(a_s x) + A(s)\exp(\beta x), \tag{4a}$$

$$\hat{T}_b(x,s) = c_3(s)\exp(-a_b|l+x|), \tag{4b}$$

$$\hat{T}_g(x,s) = c_4(s)\exp(-a_g x) + c_5(s)\exp(a_g x), \tag{4c}$$

$$\hat{T}_w(x,s) = c_6(s)\exp[-a_w(x-L)], \tag{4d}$$

where

$$A(s) = \left(\frac{\eta\alpha_s\beta I_0}{K_s}\right)\left(\frac{1-\exp(-s\tau_p)}{s(s-\alpha_s\beta^2)}\right),$$

the $c_i(s)$ contain the material parameters of the system, and $a_i = (s/\alpha_i)^{1/2}$ with $i = s, b, w,$ *and* g.

It is the temperature distribution in the gas that is responsible for the time development of the PAS signal in this model. The general expression for the Laplace transform of this temperature distribution is given below:

$$\hat{T}_g(x,s) = A(s)\{\sinh[a_g(L-x)] + D\cosh[a_g(L-x)]\} \times\left(\frac{(1+Z)\{[\exp(q)+m\exp(-q)] - (\beta/a_s)[\exp(q)-m\exp(-q)]\} + 2(\lambda-1)\exp(-\beta l)}{(1+Z)\{(S+DC)[\exp(q)+m\exp(-q)] + B(C+DS)[\exp(q)-m\exp(-q)]\}}\right), \tag{5}$$

where

$$\lambda = \frac{K_s\beta}{K_b a_b}, \quad Z = \frac{K_s a_s}{K_b a_b}, \quad q = a_s l, \quad m = \frac{1-Z}{1+Z}, \quad D = \frac{K_g a_g}{K_w a_w}, \quad B = \frac{K_g a_g}{K_s a_s} \quad C = \cosh(a_g L), \quad S = \sinh(a_g L).$$

The definitions of the quantities Z, q, m, D, and B are similar to those used in Ref. 11.

The expression can be put in the form of the Laplace space counterpart of the expression for the chopped excitation mode presented by Rosencwaig and Gersho[2] as their Eq. (13) by making the following substitutions in the above expression for $\hat{T}_g(x,s)$ and rearranging the terms:

$$b \equiv 1/Z, \quad g \equiv B, \quad r \equiv \beta/a_s = b\lambda,$$

$$\hat{T}_g(x,s) = \left(\frac{\eta\beta I_0[1-\exp(-s\tau_p)]}{SK_s(\beta^2 - a_s^2)}\right)\{\sinh[a_g(L-x)] + D\cosh[a_g(L-x)]\} \times\left(\frac{(r-1)(b+1)\exp(a_s l) - (r+1)(b-1)\exp(-a_s l) + 2(b-r)\exp(-\beta l)}{(b+1)[(1+gD)S + (D+g)C]\exp(a_s l) - (b-1)[(gD-1)S + (g-D)C]\exp(-a_s l)}\right). \tag{6}$$

This expression is more general than that in Ref. 2 in that the effects of the window are taken into account through the parameter D.

B. The time-dependent photoacoustic response

In order to obtain the expression for the photoacoustic response of a cell excited by a light pulse, the time development of the temperature profile in the gas must be converted to an average pressure in the cell. This average pressure is detected by the microphone. Under typical experimental conditions the gas in the cell may be treated as an ideal gas and from the equation of state:

$$p(x,t) = R\rho(x,t)T(x,t), \tag{7}$$

where $\rho(x,t)$ is the density of the gas in the one-dimensional enclosure and R is the gas constant. The average pressure in the chamber can be computed by taking the spatial average of $p(x,t)$. Rearranging Eq. (7) and recognizing that the spatial integral of $\rho(x,t)$ is the total mass of gas M_0 in the one-dimensional system, and therefore constant,[12,13] gives

$$\int_0^L \frac{p(x,t)}{T(x,t)}\,dx = R\int_0^L \rho(x,t)\,dx = RM_0. \tag{8}$$

For small departures from the equilibrium temperature T_0 and recognizing that in the approximation of the present model $p(x,t) = p(t)$ only, Eq. (8) becomes

$$\langle p(t)\rangle \int_0^L \frac{dx}{T_0\{1 + [T_1(x,t)/T_0]\}} = RM_0. \tag{9}$$

Expanding the denominator in terms of powers of $[T_1(x,t)/T_0] \ll 1$ and putting $\langle p(t)\rangle = p_0 + \Delta p(t)$ gives

$$\Delta p(t) = \frac{p_0}{T_0 L} \int_0^L T_1(x,t)\, dx. \tag{10}$$

Since the space and time coordinates are independent, the Laplace transform of Eq. (10) may be taken prior to the spatial integration to give

$$\int_0^\infty \exp(-st)\Delta p(t)\, dt = \frac{p_0}{T_0 L} \int_0^\infty \exp(-st) \int_0^L T_1(x,t)\, dx\, dt = \frac{p_0}{T_0 L} \int_0^L dx \int_0^\infty \exp(-st) T_1(x,t)\, dt,$$

i.e.,

$$\Delta \hat{p}(s) = \frac{p_0}{T_0 L} \int_0^L \hat{T}_1(x,s)\, dx. \tag{11}$$

Substituting for $\hat{T}_1(x,s)$ from Eq. (6) yields a general expression for the Laplace transform of the photoacoustic signal,

$$\Delta \hat{p}(s) = \left(\frac{\eta \beta I_0 p_0 [1 - \exp(-s\tau_p)]}{SK_s L \alpha_g T_0 (\beta^2 - a_s^2)}\right)[\cosh(a_g L) - 1 + D \sinh(a_g L)]$$

$$\times \left(\frac{(r-1)(b+1)\exp(a_s l) - (r+1)(b-1)\exp(-a_s l) + 2(b-r)\exp(-\beta l)}{(b+1)[(1+gD)S + (D+g)C]\exp(a_s l) - (b-1)[(gD-1)S + (g-D)C]\exp(-a_s l)}\right). \tag{12}$$

This expression has been inverted to obtain $\Delta p(t)$, the PAS response, for several special cases given below. These are grouped according to the optical opacity of the solid under consideration. Attempts to numerically integrate the Laplace transforms using the Dubner and Abate[14] technique suggested by Aamodt and Murphy[11] showed very slow convergence and were therefore discarded. The Euler transformation of Hamming[15] employed by Simon *et al.*[16] to speed up convergence resulted in expressions that were more complex than the analytical relationships from the explicit inversion of the Laplace transforms and were thus also discarded.

C. Special cases

For all of the cases considered, the quantities B and D defined above are very much smaller than unity, typically on the order of 10^{-3}. This enables the following approximations to be made in evaluating $\Delta \hat{p}(s)$:

$$\begin{aligned} &\sinh(a_g L) + D\cosh(a_g L) \simeq \sinh(a_g L), \\ &\cosh(a_g L) + D\sinh(a_g L) \simeq \cosh(a_g L), \\ &(D \pm B) \simeq D \quad \text{and} \quad (1 \pm DB) \simeq 1. \end{aligned} \tag{13}$$

In evaluating $\hat{T}(L,t)$ using Eq. (6), however, the term $D\cosh[a_g(L-x)]$ is retained to avoid the nonphysical situation of $T(L,t) = 0$ for all times.

1. Optically transparent thermally thin solids

For this case $\mu_\beta \equiv 1/\beta > l$ and $\exp(-\beta l) \simeq (1 - \beta l)$, also $\exp(-a_s l) \simeq (1 - a_s l)$. It is also assumed that the efficiency of the nonradiative processes $\eta = 1$. Under these circumstances

$$\hat{T}_g(x,s) = \left(\frac{\alpha_s \beta I_0 [1 - \exp(-s\tau_p)]}{K_s}\right)\left(\frac{\sinh(L-x)a_g + D\cosh(L-x)a_g}{s^{3/2}[s^{1/2} + \alpha_s^{1/2}/Zl]\sinh(La_g)}\right), \quad 0 \leqslant x \leqslant L. \tag{14}$$

Defining a relaxation time $\tau_l \equiv (Z^2 l^2/\alpha_s) = (K_s \rho_s c_s / K_b \rho_b c_b)(l^2/\alpha_s)$ the inverse Laplace transform of Eq. (14) gives the temperature distribution in the cell both during and after the excitation pulse. Using theorems (B1)–(B3), and C1) together with expression (A1) (see Table I) gives

TABLE I. Expressions used in Evaluating the PAS response.

$\hat{v}(s)$	$v(t)\equiv\mathcal{L}^{-1}[\hat{v}(s)]$.
(A1)[a] $\dfrac{\exp[-x(s/\alpha_g)^{1/2}]}{s^{1/2}(s^{1/2}+1/(\tau)^{1/2})}$	$2(\tau t)^{1/2} i\,\mathrm{erfc}\left(\dfrac{x}{(4\alpha_g t)^{1/2}}\right) + \tau\left\{\exp\left(\dfrac{t}{\tau}+\dfrac{x}{(\alpha_g\tau)^{1/2}}\right)\mathrm{erfc}\left[\dfrac{x}{(4\alpha_g t)^{1/2}}+\left(\dfrac{t}{\tau}\right)^{1/2}\right] - \mathrm{erfc}\left(\dfrac{x}{(4\alpha_g t)^{1/2}}\right)\right\}$
(A2) $\dfrac{1}{s^2((s)^{1/2}+1/(\tau)^{1/2})}$	$(\tau)^{1/2}\left[t-\left(\dfrac{4t\tau}{\pi}\right)^{1/2}\right]+\tau^{3/2}\left[1-\exp\left(\dfrac{t}{\tau}\right)\times\mathrm{erfc}(t/\tau)^{1/2}\right]$
(A3)[a] $\dfrac{\exp[-x(s/\alpha_g)^{1/2}]}{s^2((s)^{1/2}+1/(\tau)^{1/2})}$.	$\tau^{1/2}\left\{\mathrm{erfc}\left(\dfrac{x}{(4\alpha_g t)^{1/2}}\right)-2(t/\tau)^{1/2} i\,\mathrm{erfc}\left(\dfrac{x}{(4\alpha_g t)^{1/2}}\right) - \exp\left(\dfrac{t}{\tau}+\dfrac{x}{(\alpha_g\tau)^{1/2}}\right)\mathrm{erfc}\left[\dfrac{x}{(4\alpha_g t)^{1/2}}+\left(\dfrac{t}{\tau}\right)^{1/2}\right] + 4\left(\dfrac{t}{\tau}\right) i^2\mathrm{erfc}\left(\dfrac{x}{(4\alpha_g t)^{1/2}}\right)\right\}.$
(B1)[b] If $\mathcal{L}^{-1}\{f(s)\}=F(t)$	then $\mathcal{L}^{-1}\{\exp(-\alpha s)f(s)\}=\begin{cases}F(t-\alpha) & t>\alpha\\ 0 & t<\alpha\end{cases}$
(B2)[b] If $\mathcal{L}^{-1}\{f(s)\}=F(t)$ and $\mathcal{L}^{-1}\{g(s)\}=G(t)$	then $\mathcal{L}^{-1}\{f(s)g(s)\}=\int_0^t F(u)G(t-u)\,du$
(B3)[b] If $\mathcal{L}^{-1}\{f(s)\}=F(t)$	then $\mathcal{L}^{-1}\left\{\dfrac{f(s)}{s}\right\}=\int_0^t F(u)\,du$
(C1) $\{\sinh[L\sqrt{(s/\alpha_g)^{1/2}}]\}^{-1}=\sum_{n=0}^{\infty}\exp[-(2n+1)L(s/\alpha_g)^{1/2}]$.	(C2) $\tanh\frac{1}{2}x=1+2\sum_{n=1}^{\infty}(-1)^n\exp(-nx)$.
(D1) $\mathrm{erfc}x=1-\dfrac{2}{(\pi)^{1/2}}\sum_{n=0}^{\infty}(-1)^n\dfrac{x^{2n+1}}{(2n+1)n!}$.	(D2) $\mathrm{erfc}x=\dfrac{1}{(\pi)^{1/2}}\exp(-x^2)\left(\dfrac{1}{x}+\sum_{n=2}^{\infty}(-1)^n\dfrac{(1)(3)(5)\cdots(2n-3)}{2^{n-1}x^{2n-1}}\right)$

[a]See Ref. 17.

[b]See Ref. 18.

$$
\begin{aligned}
T_g(x,t) &= \left(\frac{\alpha_s\beta I_0\tau_l}{K_s}\right)\sum_{n=0}^{\infty}\left[(1+D)\left\{2\left(\frac{t}{\tau_l}\right)^{1/2} i\,\mathrm{erfc}\left(\frac{(2nL+x)}{(4\alpha_g t)^{1/2}}\right)+\exp\left[\left(\frac{t}{\tau_l}\right)+\left(\frac{2nL+x}{(\alpha_g\tau_l)^{1/2}}\right)\right]\mathrm{erfc}\left[\left(\frac{t}{\tau_l}\right)^{1/2}+\left(\frac{2nL+x}{\sqrt{4\alpha_g t}}\right)\right]\right.\right.\\
&\quad\left.-\mathrm{erfc}\left(\frac{(2nL+x)}{\sqrt{4\alpha_g t}}\right)\right\}-(1-D)\left\{2\left(\frac{t}{\tau_l}\right)^{1/2} i\,\mathrm{erfc}\left(\frac{[2(n+1)L-x]}{(4\alpha_g t)^{1/2}}\right)+\exp\left[\left(\frac{t}{\tau_l}\right)+\left[\frac{2(n+1)L-x}{(\alpha_g\tau_l)^{1/2}}\right]\right]\right.\\
&\quad\left.\left.\times\mathrm{erfc}\left[\left(\frac{t}{\tau_l}\right)^{1/2}+\left(\frac{2(n+1)L-x}{(4\alpha_g t)^{1/2}}\right)\right]-\mathrm{erfc}\left(\frac{[2(n+1)L-x]}{(4\alpha_g t)^{1/2}}\right)\right\}\right], \qquad \text{for } 0\leqslant x\leqslant L,\quad t<\tau_p, \qquad (15)
\end{aligned}
$$

and

$$
T_g(x,t>\tau_p)=[T_g(x,t<\tau_p)]_{t=t}-[T_g(x,t<\tau_p)]_{t=(t-\tau_p)}, \qquad \text{for } 0\leqslant x\leqslant L,\ t>\tau_p.
$$

where

$$
i\,\mathrm{erfc}x=\int_x^{\infty}\mathrm{erfc}y\,dy \qquad \text{for } 0\leqslant x\leqslant L,\ t>\tau_p.
$$

The relaxation time τ_l is a modified thermal diffusion time for the film of thickness l. For times $t\ll t_l$ the Laplace transform of the temperature distribution in the cell depends only upon β, whereas for times $t\gg t_l$ this quantity depends upon the product βl.

The pressure in the cell is obtained by simplifying the general expression for its Laplace transform using Eq. (13) and taking $\exp(-\beta l)\simeq(1-\beta l)$:

$$\Delta\hat{p}(s)=\left(\frac{\alpha_s\beta I_0 p_0(\alpha_g)^{1/2}}{T_0 L K_s}\right)\left[\frac{[1-\exp(-s\tau_p)]}{s^2(s^{1/2}+\tau_l^{-1/2})}\tanh\left(\frac{La_g}{2}\right)\right]. \tag{16}$$

This may be inverted using Eqs. (A2) and (A3), and (C2) to give

$$\Delta p(t)=\left(\frac{\alpha_s\beta I_0 p_0(\alpha_g^{1/2})\tau_l}{T_0 L K_s}\right)\left[\left(\frac{t}{(\tau_l^{1/2})}\right)-2\left(\frac{t}{\pi}\right)^{1/2}+\tau_l^{1/2}\left(1-\exp\left(\frac{t}{\tau_l}\right)\operatorname{erfc}\left(\frac{t}{\tau_l}\right)^{1/2}\right.\right.$$

$$+2\sum_{n=1}^{\infty}(-1)^n\left\{\operatorname{erfc}\left(\frac{nL}{(4\alpha_g t)^{1/2}}\right)-2\left(\frac{t}{\tau_l}\right)^{1/2} i\operatorname{erfc}\left(\frac{\mathrm{nL}}{(4\alpha_g \mathrm{t})^{1/2}}\right)-\exp\left[\left(\frac{t}{\tau_l}\right)+\frac{nL}{(\alpha_g\tau_l)^{1/2}}\right]\operatorname{erfc}\left[\left(\frac{t}{\tau_l}\right)^{1/2}+\frac{nL}{(4\alpha_g t)^{1/2}}\right]\right.$$

$$\left.\left.\left.+4\left(\frac{t}{\tau_l}\right)i^2\operatorname{erfc}\left(\frac{nL}{\sqrt{4\alpha_g t}}\right)\right\}\right)\right], \quad t<\tau_p, \tag{17}$$

and

$$\Delta p(t>\tau_p)=[\Delta p(t<\tau_p)]_{t=t}-[\Delta p(t<\tau_p)]_{t=(t-\tau_p)}, \quad t>\tau_p,$$

where

$$i^2\operatorname{erfc}x=\int_x^{\infty} i\operatorname{erfc}y\,dy.$$

As expected, the magnitude of the photoacoustic response depends directly upon β and I_0, an order of magnitude change in β producing a corresponding change in the PAS magnitude. Its time development is a rather complex function of material parameters and the cell dimensions. This expression has been evaluated numerically and results for two different film thicknesses, but the same optical absorption coefficient, cell, and material parameters are shown in Fig. 2, with the following values being used: $K_s = 84$ W/m K, $C_s = 700$ J/kg K, $\rho = 2.3$ gm/cm^3, $\alpha_s = 0.5$ cm^2/sec, $K_b = 237$ W/m K, $C_b = 90$ J/kg K, $\rho_b = 2.7$ g/cm^3, $p_0 = 1$ atm, and $\alpha_g = 0.2$ cm^2/sec. The pulse power flux was 3×10^6 W/cm^2. The cell length was chosen to be 0.1 cm for this evaluation both because it is a typical PAS cell dimension and because it limits the number of terms required in the numerical evaluation of $\Delta p(t)$.

The infinite series appearing in Eqs. (15) and (17) converge rapidly for early times t, i.e., large values of the argument, and less rapidly for later times. It was found that a maximum number of 25–30 terms was always adequate to secure independence of the numerical results from the number of terms used. In the numerical evaluation, the complementary error function was determined using the McLaurin series, Eq. (D1), for small values of the argument and the asymptotic series Eq. (D2), for large values. The transition from one approximation to the other was chosen at that value of the argument for which their numerical difference was minimum. This was found to occur for an argument of 3.9228 and the difference:

$$[\operatorname{erfc}(3.9228)]_{\text{Asymptotic}}-[\operatorname{erfc}(3.9228)]_{\text{McLaurin}}=2.677\times10^{-13}.$$

Figure 2(a) shows the response of a thin film ($l = 10^{-6}$ cm) to a square light pulse of 5.5×10^{-6}-sec duration. The temperature of the sample surface $T(0,t)$ is seen to increase during the pulse and to reach its maximum value at the end of the pusle after which it decays to the background value via heat conduction into the backing material and into the gas. The finite transport time of the thermal wave across the cell is shown by the diagram of the window temperature $T(L,t)$ which does not depart from the background value until this wave arrives and indicates a thermal diffusion velocity on

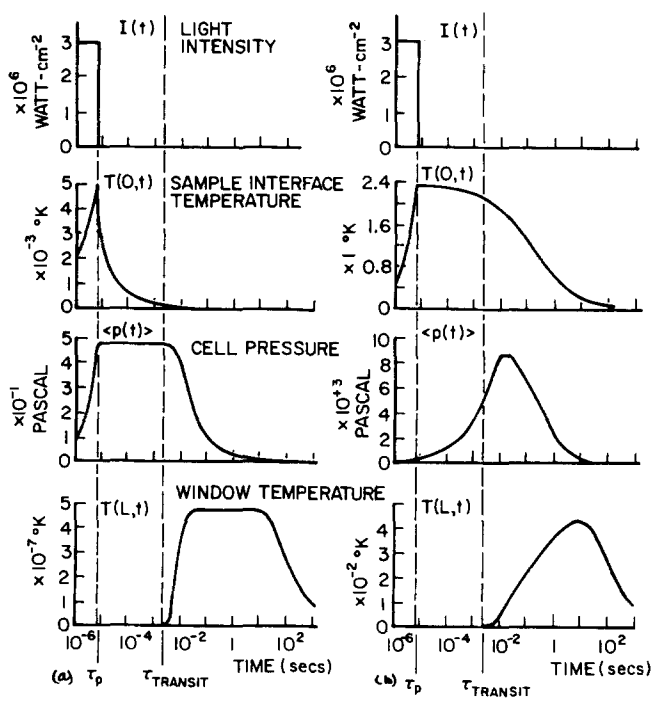

FIG. 2. Time development of cell parameters for (a) thin and (b) thick films of the same optical absorption coefficient.

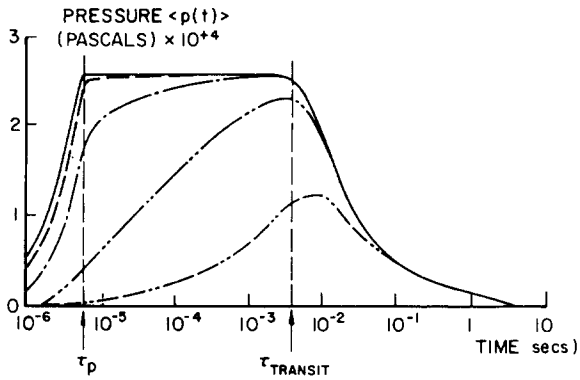

(a)

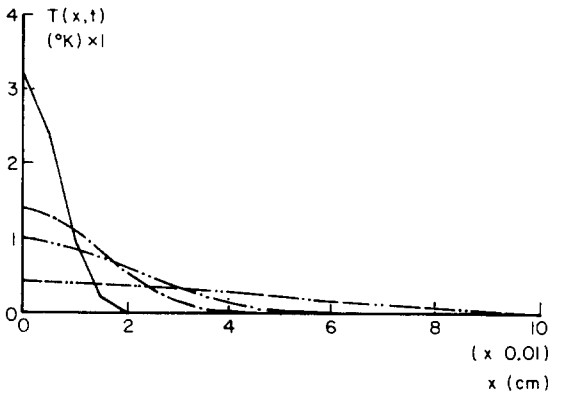

(b)

FIG. 3. (a) Dependence of the PAS signal on the value of the optical absorption coefficient for an optically thick thermally thick specimen:(—)$\beta \geqslant 10^5$ cm^{-1}, (– – –)$\beta = 10^4$ cm^{-1}, (– – –)$\beta = 10^3$ cm^{-1}, (– – – –)$\beta = 10^2$ cm^{-1}, and (– – – – – –)$\beta = 10$ cm^{-1}. (b) Temperature profile in the gas of a PAS cellat various times after the termination of the excitation pulse: (—)10^{-4} sec, (– – –) 5×10^{-4} sec, (– – – –)10^{-3} sec, and (– – – – – –)5×10^{-3} sec.

the order of 2 cm sec^{-1}. The pressure in the cell $\langle p(t)\rangle$ increases to a maximum value at the end of the pulse, remains essentially constant until the thermal wave reaches the window of the cell, and then decreases to its background value p_0 as energy is removed from the gas by transport through the window.

Figure 2(b) shows the corresponding quantities for a thick film of the same material. In this case the initial energy absorbed from the light pulse is also distributed throughout the 0.1-cm thickness of the film. The surface temperature $T(0,t)$ is still a maximum at the end of the light pulse; however, it decays to the background value much more slowly and the film transfers energy to the gas for times long compared to the thermal transit time of the gas. Because of this, the pressure in the gas does not have its maximum value at the end of the pulse but continues to increase as a function of time. The position of the maximum in the $\langle p(t)\rangle$ curve is determined by a balance between the energy transfer from the sample to the gas and energy loss from the gas through the cell window.

2. Optically opaque thermally thick solids

For this case, the optical absorption depth of the radiation is taken to be very much less than the thickness of the solid, i.e., $\mu_\beta \equiv 1/\beta \ll l$ and $\exp(-\beta l)\to 0$, also $\exp(-a_s l) \simeq 0$. Using these simplifications, the expression for the Laplace transform of the temperature distribution in the gas becomes

$$\hat{T}_g(x,s) = \left(\frac{\alpha_s \beta I_0[1-\exp(-s\tau_p)]}{K_s}\right) \times \left(\frac{\sinh(L-x)a_g + D\cosh(L-x)a_g}{s^{3/2}(s^{1/2}+\beta\alpha_s^{1/2})\sinh(La_g)}\right), 0 \leqslant x \leqslant L. \tag{18}$$

Defining a relaxation time $\tau_\beta \equiv (1/\beta^2\alpha_s)$ which corresponds to the thermal transit time from a depth μ_β in the solid indicates that for times $t \ll \tau_\beta$, $\hat{T}_g(x,s)$ exhibits a β dependence, whereas for $t \gg \tau_\beta$, $\hat{T}_g(x,s)$ exhibits no dependence on β. This is due to the fact that, in this approximation, the β occurring in the constant prefactor is cancelled by the β from the denominator of the second term when $s^{1/2}$ can be neglected compared to $\beta\alpha_s^{1/2}$.

This independence of the photoacoustic signal in the time domain from the optical absorption coefficient of the solid is exactly equivalent to the corresponding situation in the frequency domain where for high optical absorption coefficients the heat deposition profile has a range that is short compared to the thermal diffusion depth in the solid at that chopping frequency. In the time domain the corresponding thermal diffusion depth can be thought of as a time-dependent quantity increasing in magnitude as the square root of time. Once this parameter is considerably larger than the optical absorption depth in the solid β independence occurs.

$\hat{T}_g(x,s)$ can be inverted to yield the explicit relationship for the temperature distribution in the cell that is identical to Eq. (15) but with τ_l replaced by τ_β. Similarly, the expression for the pressure in the cell is identical to Eq. (17) with the same substitution being made. Figure 3(a) shows the response of a photoacoustic cell containing such an optically opaque and thermally thick sample to a pulse length of 5.5×10^{-6} sec. The different curves presented correspond to values of β ranging between 10 and 10^5 cm^{-1}. It can be seen that the PAS signal amplitude is relatively insensitive to large variations in β at experimentally attainable observation times, in contrast to the optically thin sample case, where the amplitude varies linearly with β at all times. Values of $\beta \geqslant 10^5$ cm^{-1} yield $p(t)$ curves that are identical at observation times of 10^{-6} sec or longer. If shorter observation times could be employed, the correspondingly smaller values of $\mu_s(t)$ would permit higher values of β to be resolved. It should be realized, however, that the model would break down under these conditions. All of the $p(t)$ curves decay along the same asymptote once energy leaves the cell through the window. Figure 3(b) shows the time development of the temperature profile in the gas. In contrast to the case of a temperature pulse considered by Aamodt and Murphy[11] and presented in their Fig. 7, the surface temperature of the solid does not go to zero at the end of the heating pulse. The solid surface is always the highest temperature point in the cell and the heat flux in the gas is away from this surface towards the cell

window. At times long compared to the transit time of the thermal wave, the temperature gradient in the gas is approximately linear.

Equation (18) also applies to an optically transparent thermally thick sample and to an optically opaque thermally thin sample if $b = 1$.

III. DISCUSSION

The general expression for the photoacoustic response to a pulsed excitation developed above, together with the special cases considered, indicate that the pulse technique is capable of providing useful information about the optical absorption properties of a material.

For the case of the optically transparent thin films, the characteristic relaxation time τ_l associated with the time development of the signal depends only upon the sample thickness and the thermal properties of the sample and the backing material. The information about the optical properties of the material is contained in the time-independent multiplying factor in the expression for the pressure. If observations are made at times short compared to this characteristic relaxation time, the signal depends only upon β and is independent of the sample thickness. At times larger than this characteristic time, the signal is proportional to the product βl. Recognizing the limitations of the model and taking 10^{-5} sec as the earliest practicable observation time in a gas-filled photoacoustic cell indicates that for films having thermal properties analogous to those of their support, the transition between these two regimes will only be observable for films thicker than 10^{-3} cm. For a given film thickness the time development of the PAS response will be the same for all values of β (provided $\mu_\beta > l$) but the amplitude of the signal will vary linearly with β. For films of the same β but different thicknesses, the PAS response will develop more slowly as the film thickness increases, as was indicated in Fig. 2. The maximum amplitude of the signal increases with the thickness of the film since the total energy absorbed from the incident radiation also increases.

For the thicker films, the dimensions of the photoacoustic cell become more important in controlling the time development of the signal as energy is still being transferred from the solid to the gas at times greater than the thermal diffusion time across the gas in the cell. In general, the PAS signal starts to decrease at times greater than this thermal diffusion time since the gas is losing energy to the window. The detailed form of the time response under these conditions therefore depends upon the ratio of the energy transfer to the gas from the solid and the energy loss from the gas to the window. At long times this last process dominates and all curves decay along the same asymptote to the initial temperature of the cell.

In the case of the optically and thermally thick solid, the corresponding characteristic time of the system is that for which the thermal diffusion length in the solid is equal to the optical absorption depth, i.e., $(\alpha_s \tau_\beta)^{1/2} = \mu_\beta$. Since the solid has been assumed to be thermally thick, i.e., for all times of interest $(\alpha_s t)^{1/2} < l$, the PAS response is independent of the sample thickness. The optical absorption properties of the solid are contained in both the time-independent factor and the time development of the photoacoustic signal. As expected intuitively, the photoacoustic signal develops more rapidly in a cell of fixed properties for higher optical absorption coefficients. The largest value of β that can be resolved depends upon the shortest time at which the time development of the photoacoustic signal can be followed since "β saturation" occurs at times for which the time-dependent thermal diffusion length in the solid becomes greater than the optical absorption depth (i.e., the energy deposition profile). Figure 3(a) also indicates the interplay between the energy deposition in the gas from the solid and the loss of energy from the gas through the cell window. For high optical absorption coefficients more of the absorbed energy has been transferred to the gas before heat losses occur from the cell through the window and the pressure tends to saturate before decaying to its initial value. For the lower optical absorption coefficients, heat is deposited in the gas from the solid for longer periods of time and the heat losses through the window prevent the pressure from reaching the same maximum value. This interplay between the two heat transfers causes the maximum cell pressure to be lower for solids of lower optical absorption coefficient and the maximum of $p(t)$ to occur at later times. Typically, the pressure in the cell will reach the same saturation value for samples of different β if the thermal transit time across the cell is greater than $\sim 10^3 \tau_\beta$.

Another form of time-domain saturation, "thermodynamic saturation", which also gives a response that is β independent (in the limit of the optically thick approximation) occurs when the heat losses from the cell just balance the heat imput to the solid via the optical absorption process. This form of saturation requires the establishment of time-independent temperature gradients in both the sample and the gas cell and for specimens of normal dimensions would need long-duration light pulses such as the step-function pulse considered by Aamodt and Murphy.[11]

The dependence of β saturation on the shortest possible time of observation suggests that, in order to extend time domain PAS to the highest possible values of β, a zero length cell with piezoelectric detection would be advantageous. Presumably, for the correct interpretation of the response, the interaction between the solid and the detector would have to be treated in a manner analogous to that employed by McDonald and Wetsel.[7]

Comparison of the equations for the optically and thermally thin film case and the optically and thermally thick case presented above indicates that the sample thickness in the case of the thin films plays the same role in the time development of the PAS response as does μ_β in the case of the thick films. The curves presented in fig. 2 for films of the same β but with thicknesses of 10^{-6} and 10^{-3} cm have the same form as those obtained for an optically and thermally thick solid for which $\mu_\beta = 10^{-6}$ or 10^{-3} cm. For the thin films, however, the signal magnitudes scale directly with β, whereas for the thick specimens the signal magnitude is less β dependent.

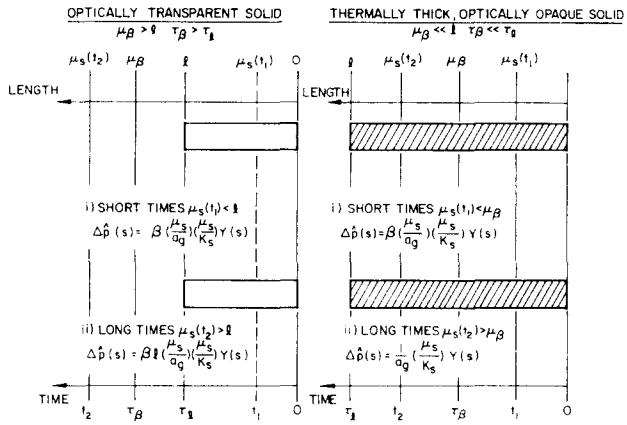

FIG. 4. Diagram showing characteristic times and lengths important in time-domain PAS. $Y(s) = (p_0 I_0/LT_0)\{[1-\exp(-s\tau_\rho)]/s\}\tanh(\frac{1}{2}L\alpha_g)$.

As indicated above, the present time-domain model in Laplace space is the equivalent of the Rosencwaig-Gersho model in the frequency domain but with each pulse displaying in the time-domain development of the photoacoustic signal that information obtainable in the modulation mode by separate measurements at different modulation frequencies. Early times correspond to high modulation frequencies and therefore contain surface information, later times provide weighted information from the interior of the samples.

In order to illustrate this point further, Fig. 4 shows the effect of the relative spatial positions of the distances l, μ_β, and $\mu_s(t) \equiv (\alpha_s t)^{1/2}$ on the form of the PAS signal for the special case considered above. The characteristic times τ_β and τ_l are shown on the corresponding time axis in Fig. 4. Transitions between approximations occur when the time-dependent thermal diffusion length $\mu_s(t)$ becomes greater than l for the case of optically transparent solids or μ_β for the optically opaque solids. A comparison of this diagram with Fig. 3 of Ref. 2 demonstrates the expected complete analogy of the time-domain PAS response to that obtainable in the frequency domain.

One of the potential advantages of time-domain photoacoustic spectroscopy is the facility with which delay times may be measured with high precision. In the present model it has been assumed that the nonradiative events providing the distributed heat source in the solid are instantaneous. The case for which these processes have a characteristic relaxation time is currently being developed using the same approximate expression for the thermal transport equation of the gas. As in the case of modulation PAS, a major problem in obtaining relaxation times is deconvoluting time delays due to optical density changes (and a concomitant change in the characteristic time for thermal transport in the solid) from those associated with the relaxation time of the nonradiative deexcitations.

ACKNOWLEDGMENTS

The authors would like to thank Professor G. Bienkowski and Professor S.H. Lam and Dr. J.J. Gelfand for useful discussions during the course of this work. Partial support by ARO Contract DAAG29-76-C-0054 is gratefully acknowledged.

[1] A. Rosencwaig and A. Gersho. Science **190**, 556 (1975).
[2] A. Rosencwaig and A. Gersho. J. Appl. Phys. **47**, 64 (1976).
[3] A. Rosencwaig, J. Appl. Phys. **49**, 2905 (1978).
[4] A. Rosencwaig, *Optoacoustic Spectroscopy and Detection*, edited by Yoh-Han Pao (Academic, New York, 1977), p. 194.
[5] J.G. Parker. Appl. Opt. **12**, 2974 (1973).
[6] L.C. Aamodt, J.C. Murphy, and J.G. Parker, J. Appl. Phys. **48**, 927 (1977).
[7] F.A. McDonald and G.C. Wetsel, J. Appl. Phys. **49**, 2313 (1978).
[8] J.B. Callis, W.W. Parson, and M. Gouterman, Biochem. Biophys. Acta **267**, 348 (1972).
[9] J.B. Callis, J. Res. Natl. Bur. Stand. A **80**, 413 (1976).
[10] M.M. Farrow, R.K. Burnham, M. Auzannean, S.L. Olsen, N. Purdie, and E.M. Eyring. Appl. Opt. **17**, 1093 (1978).
[11] L.C. Aamodt and J.C. Murphy. J. Appl. Phys. **49**, 3036 (1978).
[12] S.H. Lam (private communication).
[13] H.S. Bernnett and R.A. Forman. J. Appl. Phys. **48**, 1217 (1977).
[14] H. Dubner and J. Abate. J. Assoc. Comput. Mach. **15**, 115 (1968).
[15] R.W. Hamming. *Numerical Methods for Scientists and Engineers* (McGraw-Hill, New York, 1962).
[16] R.M. Simon, M.T. Stroot, G.H. Weiss. Comput. Biomed. Res. **5**, 595 (1972).
[17] H.S. Carlslaw and J.C. Jaeger, *Conduction of Heat in Solids* (Oxford U.P., Oxford, 1959), Appendix V.
[18] M.R. Spiegel. *Theory and Problems of Laplace Transforms* (McGraw-Hill, New York, 1965).